Structure and Magnetic Properties of CePtZn

Ratikanta Mishra[a,b], Wilfried Hermes[a], and Rainer Pöttgen[a]

[a] Institut für Anorganische und Analytische Chemie, Universität Münster,
Corrensstrasse 30, D-48149 Münster, Germany

[b] Chemistry Division, Bhabha Atomic Research Centre, Trombay, Mumbai-400 085, India

Reprint requests to R. Pöttgen. E-mail: pottgen@uni-muenster.de

The intermetallic compound CePtZn was synthesized from the elements in a sealed tantalum tube by induction melting and structurally characterized by powder and single crystal X-ray diffractometer data: TiNiSi-type, space group $Pnma$, a = 706.89(19), b = 435.08(15), c = 809.71(16) pm, $wR2$ = 0.0385, 404 F^2 values and 20 variables. The platinum and zinc atoms build up a three-dimensional network of condensed distorted $PtZn_{4/4}$ tetrahedra with Pt–Zn distances in the range 268 – 273 pm. The cerium atoms fill channels within the [PtZn] network. CePtZn shows Curie-Weiss behavior in the temperature range from 75 to 300 K with μ_{eff} = 2.47 μ_B/Ce atom and θ_P = −18.7 K, indicating trivalent cerium. No magnetic ordering was detected down to 2 K.

Key words: Intermetallics, Cerium, Magnetic Properties

Introduction

Depending on the valence electron concentration (VEC) the equiatomic cerium compounds CeTX (T = late transition metal; X = element of the 3rd, 4th, or 5th main group) reveal a variety of interesting magnetic properties. To give an example, in the series CePtIn, CePtSn to CePtSb the magnetic properties change from a heavy fermion system [1] to an 8 K [2] and 4.5 K [3] antiferromagnet. From the intermediate-valent gallide CeRhGa [4], the system changes to the 9.3 K antiferromagnet CeRhGe [5], and CeRhAs [6] is a valence-fluctuating compound. In the platinum-based series we were recently able to further reduce the VEC by substitution of indium by magnesium. In ZrNiAl-type CePtMg [7], magnesium takes part in the covalently bonded [PtMg] network and the magnetic ordering temperature is 3.6 K. Several systems like CeAuIn$_{1-x}$Mg$_x$ show complete solid solubility [8]. We have now started a more systematic investigation of the corresponding zinc-based systems, in order to elucidate similarities to the magnesium compounds. Herein we report on the synthesis, structure, and magnetic properties of CePtZn.

Experimental Section

Synthesis

Starting materials for the synthesis of CePtZn were a cerium ingot (Johnson Matthey), platinum powder (Degussa-Hüls, 200 mesh) and zinc granules (Merck), all with stated purities better than 99.9 %. Pieces of the larger cerium ingot were first arc-melted [9] to a small button under an argon atmosphere. The argon was purified before with molecular sieves, silica gel, and titanium sponge (900 K). Subsequently the cerium button, platinum powder and pieces of the zinc granules (1 : 1 : 1 atomic ratio) were sealed in a tantalum tube under an argon pressure of *ca.* 700 mbar. The tube was placed in a water-cooled sample chamber of an induction furnace (Hüttinger Elektronik, Freiburg, type TIG 1.5/300) under flowing argon [10] and was annealed at 1600 K for about five minutes, followed by slow cooling to 920 K. Finally the sample was kept at that temperature for another six hours, followed by quenching. The temperature was controlled through a Sensor Therm Methis MS09 pyrometer with an accuracy of ±30 K. The sample could easily be separated from the crucible material. No reaction with the container was observed. CePtZn is stable in air over weeks. Single crystals exhibit metallic lustre while the ground powder is grey.

EDX data

Semiquantitative EDX analyses were carried out by use of a Leica 420i scanning electron microscope with CeO$_2$, platinum, and zinc as standards. The experimentally observed composition (35 ± 2 at.-% Ce : 35 ± 2 at.-% Pt : 30 ± 2 at.-% Zn) was close to the ideal one. No impurity elements heavier than sodium (limit of the instrument) were found. The standard uncertainties account for the measurements at different points on the sample.

Table 1. Crystal data and parameters pertinent to data collection and structure refinement of CePtZn.

Empirical formula	CePtZn
Structure type	TiNiSi
Space group; Z	*Pnma*; 4
Molar mass, g mol^{-1}	400.58
Unit cell dimensions, pm	$a = 706.89(19)$
(Guinier data)	$b = 435.08(15)$
	$c = 809.71(16)$
Volume, nm^3	0.2490
ρ, g cm^{-3}	10.68
Crystal size, μm^3	$20 \times 40 \times 40$
Transm. ratio (max/min)	1.23
Radiation; wavelength, pm	MoK_α; 71.073
μ, mm^{-1}	83.1
$F(000)$, e	664
θ Range, deg	3 – 30
Range in *hkl*	$\pm 9, \pm 6, -11 - +5$
Total number of reflections	2174
Independent reflections	404 ($R_{\text{int}} = 0.0952$)
Reflections with $I \geq 2\sigma(I)$	351 ($R_\sigma = 0.0430$)
Data / refined parameters	404 / 20
Goodness-of-fit on F^2	1.109
Final *R* Indices [$I \geq 2\sigma(I)$]	$R1 = 0.0238$
	$wR2 = 0.0371$
R indices (all data)	$R1 = 0.0318$
	$wR2 = 0.0385$
Extinction coefficient	0.0081(3)
Largest diff. peak / hole, e Å^{-3}	2.08 / −2.49

X-Ray diffraction

The polycrystalline sample was studied through a Guinier powder pattern (imaging plate technique, Fujifilm BAS–1800) using Cu$K_{\alpha 1}$ radiation and α-quartz ($a = 491.30$ and $c = 540.46$ pm) as an internal standard. The orthorhombic lattice parameters (Table 1) were obtained from a least-squares fit of the powder data. To ensure proper indexing, the experimental pattern was compared to a calculated one [11] taking the atomic positions from the structure refinement. The powder and single crystal lattice parameters ($a = 706.8(1)$, $b = 434.9(1)$, $c = 809.7(1)$ pm) compared well.

Small single crystals were selected from the annealed sample and first investigated *via* Laue photographs on a Buerger camera (white Mo radiation) in order to check the quality for intensity data collection. Single crystal intensity data were collected at r. t. by use of a four-circle diffractometer (CAD4) with graphite-monochromatized MoK_α radiation and a scintillation counter with pulse height discrimination.

Table 3. Interatomic distances (pm), calculated with the powder lattice parameters of CePtZn. Standard deviations are all equal or less than 0.1 pm. All distances within the first coordination spheres are listed.

Ce:	1	Pt	296.5	Pt:	2	Zn	267.8
	2	Pt	306.2		1	Zn	272.7
	2	Pt	309.2		1	Zn	273.2
	1	Zn	316.3		1	Ce	296.5
	2	Zn	317.9		2	Ce	306.2
	2	Zn	329.8		2	Ce	309.2
	1	Zn	341.6		1	Ce	386.2
	2	Ce	365.7	Zn:	2	Pt	267.8
	2	Ce	381.8		1	Pt	272.7
	1	Pt	386.2		1	Pt	273.2
	2	Ce	435.1		1	Ce	316.3
					2	Ce	317.9
					2	Zn	322.9
					2	Ce	329.8
					1	Ce	341.6

The scans were taken in the $\omega/2\theta$ mode and an empirical absorption correction was applied on the basis of ψ-scan data, accompanied by a spherical absorption correction. All relevant details concerning the data collection are listed in Table 1.

Structure refinement

The isotypy with the orthorhombic TiNiSi-type [12], space group *Pnma*, was already evident from the powder pattern. The atomic parameters of NP-CePtSn [13] were taken as starting values and the structure was refined with full-matrix least-squares methods on F^2 using SHELXL-97 [14]. Anisotropic atomic displacement parameters were used for all atoms. As a check for the correct composition, the occupancy parameters of all sites were refined in separate series of least-squares cycles. All sites were fully occupied within two standard deviations, and in the final cycles the ideal occupancy parameters were assumed again. The final difference Fourier synthesis was flat (Table 1). The positional parameters and interatomic distances are listed in Tables 2 and 3. Further details of the crystal structure investigation may be obtained from Fachinformationszentrum Karlsruhe, 76344 Eggenstein-Leopoldshafen, Germany (fax: +49-7247-808-666; e-mail: crysdata@fiz-karlsruhe.de, http://www.fiz-informationsdienste.de/en/DB/icsd/depot_anforderung.html) on quoting the deposition number CSD-418546.
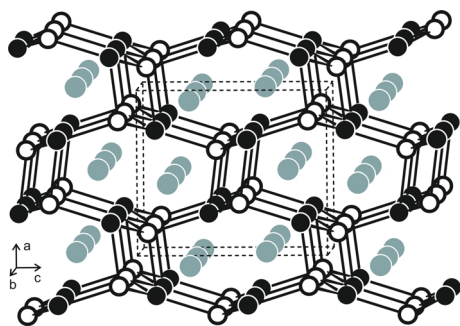
Table 2. Atomic coordinates and anisotropic displacement parameters (pm^2) of CePtZn. All atoms lie on Wyckoff positions $4c$ (x, $1/4$, z). U_{eq} is defined as one third of the trace of the orthogonalized U_{ij} tensor. The anisotropic displacement factor exponent takes the form: $-2\pi^2[(ha^*)^2 U_{11} + \ldots + 2hka^*b^* U_{12}]$. $U_{12} = U_{23} = 0$.

Atom	x	z	U_{11}	U_{22}	U_{33}	U_{13}	U_{eq}
Ce	0.02971(9)	0.69197(8)	101(3)	97(3)	97(3)	−5(2)	98(2)
Pt	0.26669(6)	0.38992(5)	104(2)	90(2)	110(2)	13(2)	102(1)
Zn	0.14950(19)	0.06837(16)	123(6)	98(6)	81(6)	17(5)	101(3)

Fig. 1. The crystal structure of CePtZn as viewed approximately along the *b* axis. The cerium, platinum, and zinc atoms are drawn as medium grey, black, and open circles, respectively. The three-dimensional [PtZn] network is emphasized.
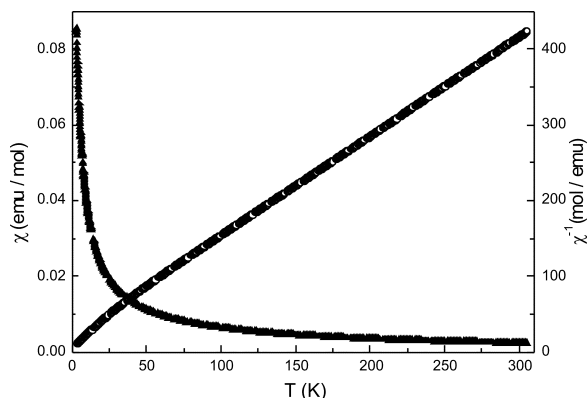

Fig. 2. Temperature dependence of the magnetic (χ) and the inverse magnetic susceptibility (χ^{-1}) of CePtZn measured at an external flux density of 10 kOe.
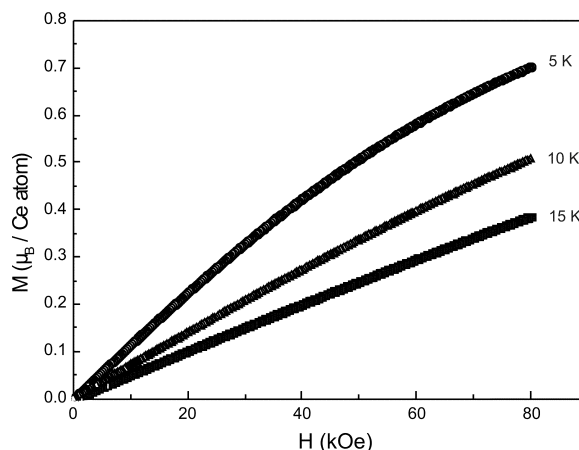

Fig. 3. Magnetization *vs.* external magnetic flux density of CePtZn at 5, 10, and 15 K.
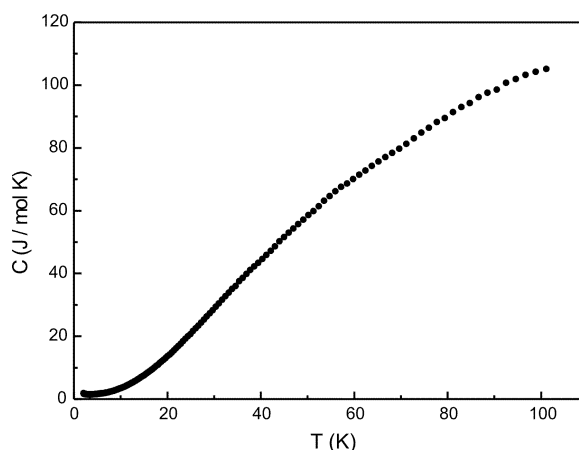
Fig. 4. Temperature dependence of the specific heat of CePtZn measured in zero magnetic field.

Susceptibility measurements

The CePtZn sample was packed in kapton foil and attached to the sample holder rod of a VSM for measuring the magnetic properties in a Quantum Design Physical-Property-Measurement-System in the temperature range 3 – 320 K with magnetic flux densities up to 80 kOe. For heat capacity (C_p) measurements (2 – 100 K) the sample was glued to the platform of a pre-calibrated heat capacity puck using Apiezon N grease.

Discussion

CePtZn is a new compound in the series of Ce*TX* intermetallics. A view of the CePtZn structure approximately along the *b* axis is shown in Fig. 1. CePtZn crystallizes with the orthorhombic TiNiSi-type structure [12], space group *Pnma*. The platinum atoms have distorted tetrahedral zinc coordination at

Pt–Zn distances ranging from 268 to 273 pm, somewhat longer than the sum of the covalent radii of 254 pm [15]. These tetrahedra are condensed *via* all corners leading to a three-dimensional [PtZn] network in which the cerium atoms fill channels. Bonding of the cerium atoms to the network proceeds *via* short Ce–Pt distances (297 – 309 pm), even shorter than in isotypic NP-CePtSn [13]. Since the crystal chemistry and chemical bonding of TiNiSi-type intermetallic compounds have been discussed in detail in different reviews [16 – 20], we refer to the literature for further information.

The temperature dependence of the inverse magnetic susceptibility of CePtZn is shown in Fig. 2. CePtZn shows Curie-Weiss behavior in the temperature range 75 – 300 K. A fit of the susceptibility data in

this temperature range results in an effective magnetic moment of $\mu_{\text{eff}} = 2.47\ \mu_B$/Ce atom and a paramagnetic Curie temperature of $\theta_P = -18.7$ K. The experimental moment is close to the free ion value of 2.54 μ_B for Ce^{3+}, indicating trivalent cerium in CePtZn. The magnetic data gave no hint for magnetic ordering down to 3 K. The small deviation from Curie-Weiss behavior at low temperatures is most likely due to crystal field splitting of the $J = 5/2$ ground state of cerium. The magnetization isotherms at 5, 10, and 15 K are shown in Fig. 3. At 10 and 15 K, the magnetization increases almost linearly, as expected for a paramagnetic material. At 5 K the magnetization shows a steeper increase, however, we do not observe saturation at the highest obtainable field of 80 kOe. The magnetization at 5 K and 80 kOe is only 0.70(1) μ_B/Ce atom, significantly reduced from the theoretical value for Ce^{3+} of 2.14 μ_B. Similar magnetic behavior has been observed for HP-CePtSn [13] and $CeRhSn_2$ [21]. Specific heat data of CePtZn were recorded down to 2 K (Fig. 4). There was no hint for a λ-type anomaly down to the lowest obtainable temperature.

[1] H. Fujii, Y. Uwatoko, M. Akayama, K. Satoh, Y. Maeno, T. Fujita, J. Sakurai, H. Kamimura, T. Okamoto, *Jpn. J. Appl. Phys.* **1987**, *Vol. 26, Suppl. 26–3*, 549.

[2] J. Sakurai, Y. Yamaguchi, S. Nishigori, T. Suzuki, T. Fujita, *J. Magn. Magn. Mater.* **1990**, *90&91*, 422.

[3] M. Kasaya, H. Suzuki, T. Yamaguchi, K. Katoh, *J. Phys. Soc. Jpn.* **1992**, *61*, 4187.

[4] F. Hulliger, *J. Alloys Compd.* **1996**, *239*, 131.

[5] P. Rogl, B. Chevalier, M. J. Besnus, J. Etourneau, *J. Magn. Magn. Mater.* **1989**, *80*, 305.

[6] K. Uemo, K. Masumori, T. Sasakawa, F. Iga, T. Takabatake, Y. Ohishi, T. Adachi, *Phys. Rev. B* **2005**, *71*, 064110.

[7] B. J. Gibson, A. Das, R. K. Kremer, R.-D. Hoffmann, R. Pöttgen, *J. Phys.: Condens. Matter* **2002**, *14*, 5173.

[8] S. Rayaprol, B. Heying, R. Pöttgen, *Z. Naturforsch.* **2006**, *61b*, 495.

[9] R. Pöttgen, Th. Gulden, A. Simon, *GIT Labor-Fachzeitschrift* **1999**, *43*, 133.

[10] D. Kußmann, R.-D. Hoffmann, R. Pöttgen, *Z. Anorg. Allg. Chem.* **1998**, *624*, 1727.

[11] K. Yvon, W. Jeitschko, E. Parthé, *J. Appl. Crystallogr.* **1977**, *10*, 73.

[12] C. B. Shoemaker, D. P. Shoemaker, *Acta Crystallogr.* **1965**, *18*, 900.

[13] J. F. Riecken, G. Heymann, T. Soltner, R.-D. Hoffmann, H. Huppertz, D. Johrendt, R. Pöttgen, *Z. Naturforsch.* **2005**, *60b*, 821.

[14] G. M. Sheldrick, SHELXL-97, Program for Crystal Structure Refinement, University of Göttingen, Göttingen (Germany) **1997**.

[15] J. Emsley, *The Elements*, Oxford University Press, Oxford **1999**.

[16] G. Nuspl, K. Polborn, J. Evers, G. A. Landrum, R. Hoffmann, *Inorg. Chem.* **1996**, *35*, 6922.

[17] G. A. Landrum, R. Hoffmann, J. Evers, H. Boysen, *Inorg. Chem.* **1998**, *37*, 5754.

[18] R.-D. Hoffmann, R. Pöttgen, *Z. Kristallogr.* **2001**, *216*, 127.

[19] M. D. Bojin, R. Hoffmann, *Helv. Chim. Acta* **2003**, *86*, 1653.

[20] M. D. Bojin, R. Hoffmann, *Helv. Chim. Acta* **2003**, *86*, 1683.

[21] D. Niepmann, R. Pöttgen, B. Künnen, G. Kotzyba, C. Rosenhahn, B. D. Mosel, *Chem. Mater.* **1999**, *11*, 1597.